Cell Reports
Report

Unique Preservation of Neural Cells in Hutchinson-Gilford Progeria Syndrome Is Due to the Expression of the Neural-Specific miR-9 MicroRNA

Xavier Nissan,[1,*] Sophie Blondel,[2,3] Claire Navarro,[4] Yves Maury,[1] Cécile Denis,[1] Mathilde Girard,[1] Cécile Martinat,[2,3] Annachiara De Sandre-Giovannoli,[4,5] Nicolas Levy,[4,5] and Marc Peschanski[1,2,3]
[1]CECS
[2]INSERM U-861
[3]UEVE U-861
I-STEM, AFM, Institute for Stem Cell Therapy and Exploration of Monogenic Diseases, 5 rue Henri Desbruères, 91030 Evry cedex, France
[4]AMU-INSERM UMR_S 910 Génétique médicale et génomique fonctionnelle, Faculté de Médecine la Timone, 27 Boulevard Jean Moulin, 13385 Marseille, France
[5]Département de Génétique Médicale, Hôpital d'Enfants la Timone, 264 Rue St. Pierre, 13385 Marseille, France
*Correspondence: xnissan@istem.fr
DOI 10.1016/j.celrep.2012.05.015

SUMMARY

One puzzling observation in patients affected with Hutchinson-Gilford progeria syndrome (HGPS), who overall exhibit systemic and dramatic premature aging, is the absence of any conspicuous cognitive impairment. Recent studies based on induced pluripotent stem cells derived from HGPS patient cells have revealed a lack of expression in neural derivatives of lamin A, a major isoform of *LMNA* that is initially produced as a precursor called prelamin A. In HGPS, defective maturation of a mutated prelamin A induces the accumulation of toxic progerin in patient cells. Here, we show that a microRNA, miR-9, negatively controls lamin A and progerin expression in neural cells. This may bear major functional correlates, as alleviation of nuclear blebbing is observed in nonneural cells after miR-9 overexpression. Our results support the hypothesis, recently proposed from analyses in mice, that protection of neural cells from progerin accumulation in HGPS is due to the physiologically restricted expression of miR-9 to that cell lineage.

INTRODUCTION

Hutchinson-Gilford progeria syndrome (HGPS or progeria) is an extremely rare disease characterized by phenotypic features of premature and accelerated aging in children (Hennekam, 2006). HGPS is typically caused by a de novo transition (c.1824C > T) in *LMNA* (De Sandre-Giovannoli et al., 2003; Eriksson et al., 2003), encoding major components of the nuclear lamina, the lamins A and C (Burke and Stewart, 2006). While apparently silent (p.G608G), the HGPS mutation activates a cryptic splicing site leading to the production and accumulation of progerin, a truncated form of prelamin A, the lamin A precursor (De Sandre-Giovannoli et al., 2003; Eriksson et al., 2003). Progerin is aberrantly farnesylated and leads to various subcellular abnormalities when it accumulates in HGPS nuclei. These defects include misshapen nuclei, changes in spatial distribution of nuclear pore complexes (Goldman et al., 2004), chromatin disorganization (Columbaro et al., 2005), genomic instability (Liu et al., 2005), and premature cell senescence (Navarro et al., 2006). HGPS-affected patients develop cardiovascular disease, heart failure, and stroke, uniformly leading to death at a mean age of 13 years old. While most of the tissues and organs are affected with defects reminiscent of aging (Merideth et al., 2008), it is intriguing that cognitive functions are preserved, suggesting a remarkable sparing of central nervous system through the entire patient's life course. The molecular bases have been sought here, by taking the opportunity of obtaining neural cells in vitro from patients affected with HGPS through derivation of induced pluripotent stem cells (iPSC).

Over the past 10 years, molecular mechanisms of HGPS have mostly been approached in vitro using peripheral cells—genetically modified or not—issued from skin, blood, or bone marrow (Misteli and Scaffidi, 2005; Paradisi et al., 2005). In several instances, these cells were not directly relevant for extrapolation to the behavior of other cell types, especially neural cell lineages. Meanwhile, previous reports had revealed the absence of lamin A expression in chicken and mouse embryonic brains (Lehner et al., 1987; Röber et al., 1989). The recent emergence of the iPSC technology has rapidly prompted the derivation of a number of cell lines derived from HGPS patients, increasing considerably the number of cell types of interest (Ho et al., 2011; Liu et al., 2011a, 2011b; Zhang et al., 2011). Among them, a particular focus was set to neural cells that have allowed authors to confirm, in humans, the absence of a significant expression of lamin A in cells of the neural lineage in vitro, and, as an expected functional correlation, the subsequent lack of nuclear blebbing (Zhang et al., 2011). However, molecular mechanisms at the origin of this specific preservation of cells of the neural lineage still remain to be elucidated. Recently, Loren Fong and colleagues have gone one step further by proposing miR-9 as

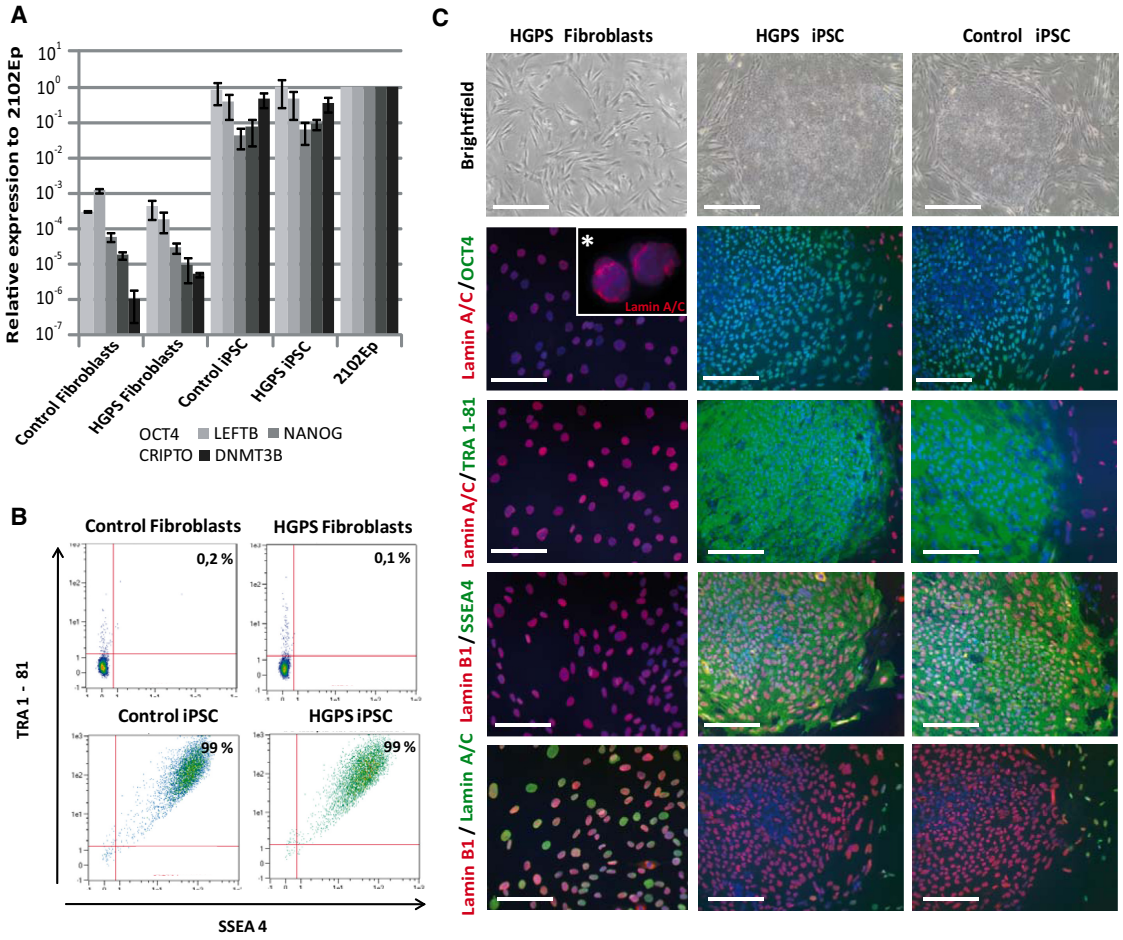

Figure 1. Molecular Characterization of Control and HGPS iPSC

(A) qRT-PCR analysis of pluripotency and self-renewal markers OCT4, LEFTB, NANOG, CRIPTO, DNMT3B in control and HGPS fibroblasts and iPSC. Data are normalized on teratocarcinoma cells (EP2102). Each histogram represents the means ± SD of three independent experiments.

(B) Flow cytometry analysis of pluripotency and self-renewal markers TRA 1-81 and SSEA4 in fibroblasts in control and HGPS fibroblasts and iPSC. Values indicate means ± SD of three independent experiments.

(C) Immunostaining of lamin A/C (JOL2 and ab8984 antibodies) and lamin B1 and pluripotency and self-renewal markers OCT4, TRA 1-81, and SSEA4 in HGPS fibrobasts, undifferentiated control and HGPS iPSC. *Boxes represent higher magnification. Scale bar is 50 μm.

See also Figure S1.

a potential regulator of lamin A expression in mouse neural cells (Jung et al., 2012). These authors have associated the absence of lamin A in murine neurons to a regulation by microRNAs and identified miR-9, a neural specific microRNA, as an effective regulator. Here, we have extended those results to neural precursors and neurons of HGPS patients, using the iPSC technology.

RESULTS

iPSC were generated from HGPS and control patients fibroblasts (Figures 1A and 1B). As previously described, A-type lamins were absent from undifferentiated iPSC (Figure 1C). In contrast, their expression was observed in a variety of iPSC-derived cells including keratinocytes, melanocytes, retinal pigment epithelial cells, and mesenchymal stem cells (MSC-iPSC) (Figures 2A and 2B; Table S1). Because MSC derived from HGPS iPSC presented the commonly described abnormalities of HGPS iPSC derivatives, namely, loss of proliferation capacities, premature senescence and nuclear blebbing (Figures S1A–S1E), we have used, thereafter, these cells as a "positive control" for comparison with cells of neural lineages. Differentiation of iPSC along the neural lineage was obtained for both control and HGPS cell lines, up to near-homogeneity following their differentiation into neural stem cells (NSC-iPSC), and after terminal differentiation into telencephalic neurons (Neurons-iPSC) (Figures S2A–S2C). Immunostaining and flow cytometry analysis using both anti-lamins A/C and specific anti-lamin A antibodies, confirmed the absence of these lamins in NSC-iPSC in contrast to a high expression of lamin B1 (Figures 2A and 2B and Figure S2D). The lack of lamins A/C appeared in neurons of different subtypes, as demonstrated by specifically

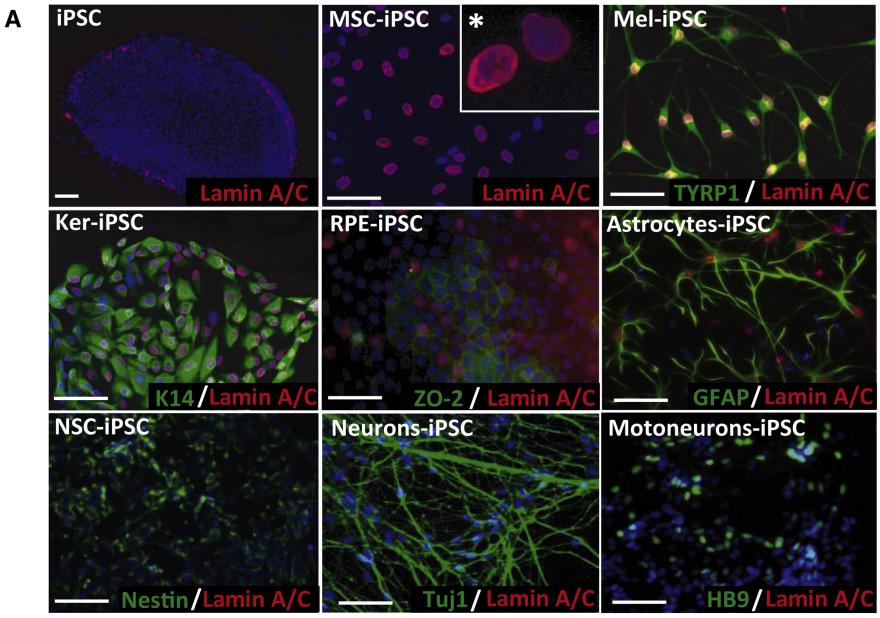

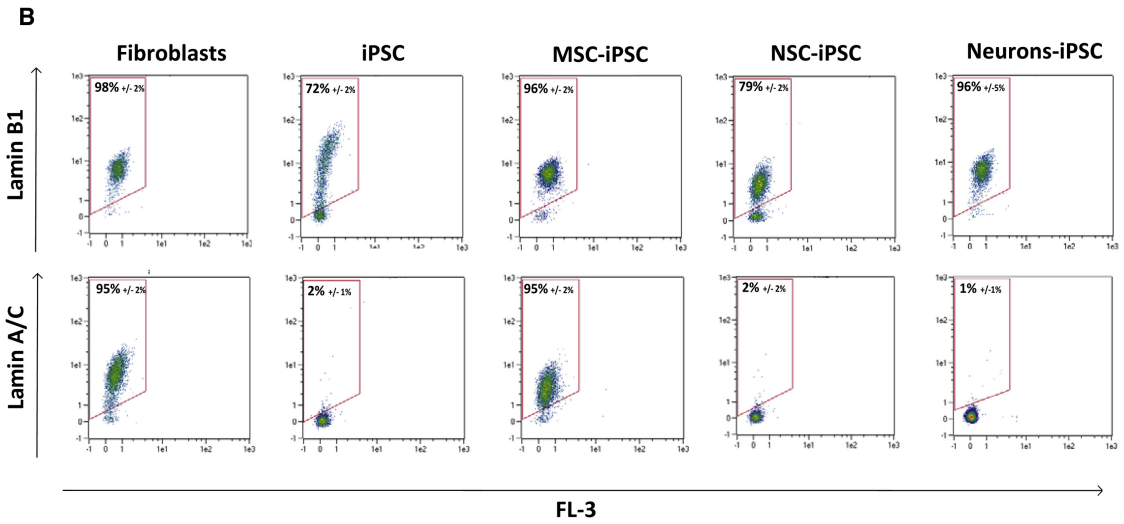

Figure 2. Characterization of Lamins Expression Profile in iPSC Derivatives

(A) Lamin A/C immunostaining (JOL2 antibody) in HGPS fibrobasts, undifferentiated HGPS iPSC and its derivatives into mesenchymal stem cells (MSC-iPSC), melanocytes (Mel-iPSC), keratinocytes (Ker-iPSC), retinal pigment epithelial cells (RPE-iPSC), astrocytes (Astrocytes-iPSC), neural stem cells (NSC-iPSC), neurons (Neurons-iPSC) and motoneurons (Motoneurons-iPSC). *Boxes represent higher magnification. Scale bar is 50 μm.

(B) Flow cytometry analysis of lamin A/C (JOL2 antibody) and lamin B1 expression in fibroblasts, iPSC, MSC-iPSC, NSC-iPSC and Neurons-iPSC. Values indicate means ± SD of three independent experiments.

See also Figure S2.

differentiating iPSC into motoneurons, but did not extend to other neural derivatives, such as astrocytes (Figure 2A).

Our study was built on the working hypothesis of an involvement of microRNAs in the neural protection observed in progeria. As a first step, three different prediction software (Target Scan, miRDB, and miRanda) were combined in order to align the lamin A 3′ untranslated region (UTR) sequence with all known microRNAs seed sequences. Computational alignments have identified two microRNAs that were candidates for targeting the lamin A 3′ UTR but not lamin C 3′ UTR: miR-129-5p and miR-9 (Figure 3A; Figures S3A and S3B). The latter has immediately attracted our attention as this microRNA is considered as the key player in neural development (Leucht et al., 2008; Yoo et al., 2009) and neural cell behavior (Ambasudhan et al., 2011; De

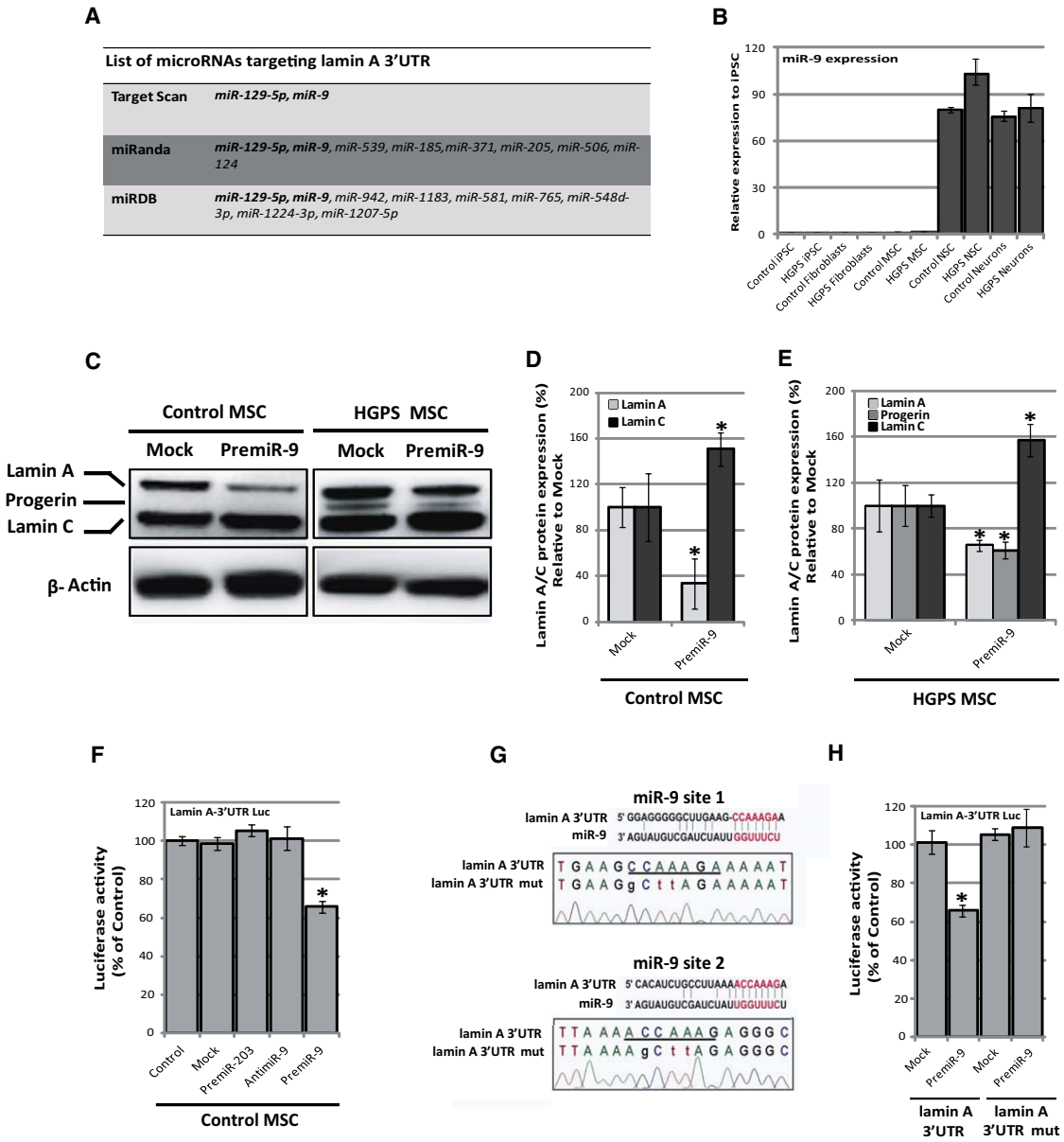

Figure 3. miR-9 Regulates Lamin A and Progerin Expression

(A) Predictive alignment of microRNAs potentially targeting the 3′ UTR sequence of lamin A using three independent algorithms: TargetScan, miRanda, and miRDB.

(B) qRT-PCR analysis of miR-9 in control and HGPS iPSC, fibroblasts, MSC-iPSC, NSC-iPSC, and Neurons-iPSC. Values represent the means ± SD of three independent experiments.

(C) Western blot analysis of lamin A/C (JOL2 antibody) and β-actin expression in control and HGPS MSC-iPSC transfected with a premiR control (Mock) or premiR-9.

(D) and (E) Quantification by western blot analysis of lamin A/C and β-Actin expression in control and HGPS MSC-iPSC transfected with a premiR control (Mock) or premiR-9. *p value < 0.05.

(F) Luciferase activity of control MSC-iPSC transfected or not with lamin A-Luc 3′ UTR plasmid in presence of a premiR control (Mock), premiR-203, anti-miR-9, or premiR-9. *p value < 0.05.

(G) Sequences alignment of the normal and mutated lamin A 3′ UTR.

(H) Luciferase activity of control MSC-iPSC transfected or not with the normal or mutated lamin A-Luc 3′ UTR plasmids in presence of a premiR control (Mock) or premiR-9. Values represent the means ± SD of three independent experiments. *p value < 0.05.

See also Figure S3.

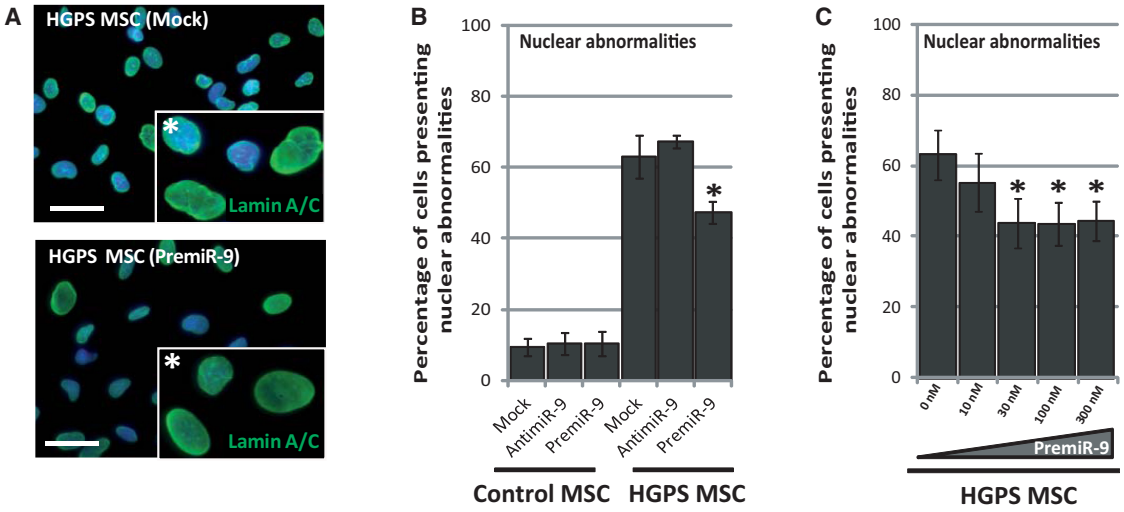

Figure 4. miR-9 Mediated Improvement of HGPS Nuclear Abnormalities

(A) Lamin A/C immunostaining (JOL2 antibody) in HGPS MSC-iPSC transfected with a premiR control (Mock) or premiR-9. *Boxes represent higher magnification. Scale bar is 50 μm.

(B) Quantification of nuclear abnormalities (lamin A/C immunostaining with JOL2 antibody) in HGPS MSC-iPSC transfected with a premiR control (Mock) or premiR-9. Values represent the means ± SD of two hundreds nuclei in three independent experiments. *p value < 0.05.

(C) Quantification of nuclear abnormalities HGPS MSC-iPSC transfected with increasing concentrations of premiR-9. Values represent the means ± SD of 200 nuclei in three independent experiments. *p value < 0.05.

See also Figure S4.

Pietri Tonelli et al., 2008; Delaloy et al., 2010; Zhao et al., 2009). We therefore dedicated further experiments toward validating the potential involvement of miR-9. Accordingly, quantitative real-time PCR (qRT-PCR) revealed that miR-9 was consistently expressed in NSC-iPSC and Neurons-iPSC, but not in fibroblasts, undifferentiated iPSC or MSC-iPSC (Figure 3B). In order to demonstrate the functional impact of miR-9 on lamins A/C expression and HGPS molecular defects, gain- and loss-of-function experiments using premiRs and anti-miRs were performed in MSC-iPSC. These cells were used to avoid any bias caused by a potential variation in endogenous miR-9 content since they do not physiologically express miR-9 and, in contrast, strongly express lamins A/C. Western blot quantification of A-type lamins revealed that, as compared to untreated controls, premiR-9 transfected cells, that overexpressed the microRNA, exhibited a decrease of 66% in the lamin A protein content. This negative regulation was specific to lamin A because, in contrast, lamin C exhibited a 50% increase under treatment with premiR-9 (Figures 3C and 3D). The same experiments were carried out in HGPS MSC-iPSC providing similar results, with miR-9 overexpression eliciting a 35% decrease in lamin A and a 55% increase in lamin C. The overexpression of miR-9 additionally promoted a 38% decrease in progerin expression in affected cells (Figure 3E). In a search for molecular mechanisms of action, the direct targeting of miR-9 on lamin A 3′ UTR was confirmed and quantified by transfecting MSC-iPSC with a plasmid that contained a luciferase gene under the control of the lamin A 3′ UTR. Measures of luminescence were performed 72 hr after co-transfection with either a premiR or anti-miR for miR-9 revealing that overexpression of miR-9 microRNA was sufficient on its own to decrease the luciferase activity by up to 40% as compared to controls and anti-miR-9-treated MSC-iPSC (Figure 3F). As a control of miR-9 specificity, the two lamin A 3′ UTR sites targeted by miR-9 were mutated, and no effect of miR-9 overexpression was then recorded (Figures 3G and 3H).

In the literature, decrease of progerin expression has been associated with a decrease in nuclear blebbing in patients' cells (Cao et al., 2011; Huang et al., 2005; Osorio et al., 2011). Accordingly, quantification of lamins A/C immunostaining revealed that whereas 60% of control and anti-miR-9 treated HGPS MSC-iPSC presented abnormally shaped nuclei, the overexpression of miR-9 induced a significant decrease of bleb containing nuclei to 48% (Figures 4A, 4B, and S4A). This effect was dose-dependent, as shown by transfecting cells with premiR-9 at successively higher concentrations (Figures 4C, S4B, and S4C).

DISCUSSION

Altogether, our results shed light on a unique molecular mechanism that specifically protects neurons in patients with Hutchinson-Gilford progeria syndrome from the defective prelamin A processing. MicroRNAs play key roles in the specific differentiation and maturation of cells and tissues in various systems (Houbaviy et al., 2003; Judson et al., 2009; Krichevsky et al., 2006; Lee et al., 1993; Ruvkun, 2001; Smirnova et al., 2005; Suh et al., 2004) including pluripotent stem cells commitment as we recently demonstrated for miR-203 in the early stages of keratinocytes development (Nissan et al., 2011a) or for miR-125 in neural differentiation (Boissart et al., 2012). These data

are consistent with the strict neural specificity of miR-9 during the first steps of mouse brain development (Smirnova et al., 2005), as well as during neural differentiation from ES cells in the mouse (Krichevsky et al., 2006) as in the Human (Delaloy et al., 2010). Over the past few years, several functional studies highlighted not only the neural-specific expression of miR-9, but its key role in the regulation of numerous processes related to neural differentiation (Zhao et al., 2009), proliferation, and migration (Delaloy et al., 2010). On the basis of these observations and according to the established key role of miR-9 in neural development, we hypothesized and demonstrated that this microRNA regulates lamin A expression in neural progenies, providing insight into the tissue selectivity of HGPS.

Our data correlate to the recently emitted hypothesis that miR-9 regulates mouse prelamin A expression revealing moreover that this molecular mechanism is conserved in humans and acts as a protective mechanism of HGPS neurons. In this context, lamin A gene extinction would physiologically be part of that general "neuralizing activity" of miR-9 showing that the singular molecular constitution of neural cells' nuclear envelope is, by itself, sufficient to significantly reduce the occurrence of dysmorphic nuclei that are otherwise elicited by the HGPS mutation in most cells. As it was previously described (Zhang et al., 2011), lamins A/C were, however, also absent from undifferentiated iPSC, i.e., in the absence of a significant expression of miR-9, suggesting the existence of others molecular regulators of A-type lamins expression in pluripotent stem cells. On the basis of our findings, we propose miR-9 as a member of the emerging list of microRNAs that have been associated with HGPS pathophysiology. In fact, recently, Carlos López-Otín and colleagues have shown that miR-1 expression was upregulated in HGPS fibroblasts, impacting cell function by reducing IGF-1 synthesis and causing a dysregulation of this major life span regulator (Mariño et al., 2010). Similarly, another family of microRNA, miR-29, was shown to be upregulated in *Zmpste24*$^{-/-}$ progeroid mice, altering the activity of Ppm1d phosphatase, which in turn enhanced p53 activity (Ugalde et al., 2011). Compared to these data, miR-9 has clearly a unique function as it impacts the disease cell phenotype at physiological levels, protecting changes in one specific cellular lineage. We thus speculate that the absence of cognitive impairment in children affected by progeria is due to a beneficial effect of miR-9 as a specific and physiological regulator of neural development. Such relations between microRNAs specificity and diseases may be applied to other metabolic diseases and other tissues, in which microRNAs similarly play key roles in the control of organogenesis (Bartel, 2009; Lee et al., 2004).

Over the years, several studies have highlighted the existence of a small number of tissue-specific microRNAs that are key players during development in vertebrates, including miR-203 for the entire sequence of skin embryogenesis (Nissan et al., 2011a; Yi et al., 2006, 2008), miR-1 and miR-133 in muscle formation (Townley-Tilson et al., 2010) as well as miR-155 and miR-181 in hematopoietic differentiation (Vasilatou et al., 2010). Whereas potential roles of microRNAs in the expression of a pathology are currently being investigated, our results support a complementary approach in the search for protective mechanisms, in particular when tissues or organs seem to be specifically unaffected by supposedly ubiquitously expressed pathological agents, as illustrated by the example of progeria.

EXPERIMENTAL PROCEDURES

Fibroblasts Reprogramming

Fibroblasts used in this study were isolated from patient biopsies performed in the Assistance Publique Hôpitaux de Marseille (13-5968, 13-8243) or provided by Coriell Institute (Camden, USA) (DM4603 and AG11513, AG01972). One control (DM4603) and two HGPS (AG01972 and 13-8243) cell lines were successfully reprogrammed to iPSC whereas the most affected HGPS cells were not (13-5968, AG11513). Three independent iPSC lines were derived from one control (DM4603) and one HGPS (13-8243) from patients using Yamanaka's original method with OCT4, KLF4, SOX2, c-Myc, transferred using retroviral vectors (Takahashi et al., 2007). The iPSC lines were amplified up to the 15th passage before differentiation.

Pluripotent Stem Cells Culture and Differentiation

Control and HGPS iPSC as well hESC from two cell lines, SA01 (Cellartis, Götenborg, Sweden) and H9 (Wicell, Madison, WI) were grown on STO mouse fibroblasts, inactivated with 10 mg/ml mitomycin C, seeded at 30000/cm^2 and grown as previously described (19). For differentiation, hESC and iPSC were differentiated into mesenchymal stem cells (MSC-iPSC) keratinocytes (Ker-iPSC), melanocytes (Mel-iPSC), and retinal pigment epithelial cells (RPE iPSC) using directed protocols for differentiation previously published by our group (Giraud-Triboult et al., 2011; Guenou et al., 2009; Nissan et al., 2011b). Neuronal differentiation was performed according to an adaptation of the dual SMAD inhibitor cocktail (Noggin, SB431542) described by Chambers and colleagues (Chambers et al., 2009). For amplification, NSC-iPSC were cultivated in N2B27 medium (Invitrogen, Carlsbad, CA) supplemented with FGF2, EGF, and brain-derived neurotrophic factor (BDNF) for 10–20 passages and terminally differentiated in the neurons-iPSC after 21 days of starvation with the mitotic growth factors (FGF2 and EGF). For motoneurons differentiation, embryoid bodies (EBs) were generated in presence of the SMAD inhibitors and caudalized by addition of retinoic acid, BDNF, ascorbic acid. After 11 days EBs were treated with Sonic Hedgehog and after 21 days cells were dissociated to be cultured up to 30 days in presence of the same medium supplemented with Rock inhibitor and glial cell line-derived neurotrophic factor (GDNF). For astrocytes generation, inhomogeneous population of motoneurons were then switched to N2B27 medium supplemented with ascorbic acid, BDNF, GDNF, and ciliary neurotrophic factor for an additional 10 days.

mRNA Purification and qRT-PCR

Total RNA from pluripotent stem cells and their derivatives were isolated using an RNeasy Mini extraction kit (QIAGEN, Courtaboeuf, France) according to the manufacturer's protocol. An on-column DNase I digestion was performed to avoid genomic DNA amplification. RNA level and quality were checked using the Nanodrop technology. A total of 500 ng of RNA was used for reverse transcription using the Superscript III reverse transcription kit (Invitrogen). qRT-PCR analysis was performed using a LightCycler 480 system (Roche, Basel Switzerland) and SYBR Green PCR Master Mix (Roche) following the manufacturer's instructions. Quantification of gene expression was based on the DeltaCt Method and normalized to 18S expression. PCR primers are listed in Table S2.

MicroRNAs Extraction and TaqMan Assay

MicroRNAs were extracted using miRVana extraction kit (Applied Biosystems, Foster City, USA) according to the manufacturer's protocol after phenol-chloroform and column purification. Individual TaqMan microRNA assays were performed on ABI 7900 (Applied Biosystems) with a no UNG no Amperase master mix (Applied Biosystems) according to the manufacturer's protocol. Results were normalized against RNU 48 a small nucleolar RNAs (snoRNAs).

Immunocytochemistry

Cells were fixed in 4% paraformaldehyde (15 min, room temperature) before permeabilization and blocking in PBS supplemented with 0.1% Triton X-100 and 1% BSA (Sigma-Aldrich, St. Louis, MO). Primary antibodies were incubated 1 hr at room temperature in blocking buffer. Antibodies included mouse anti-lamin A/C (JOL2, Millipore, Billerica, MA), rabbit anti-lamin A/C (ab8984, Abcam, Cambridge, UK), rabbit anti-lamin A (Santa Cruz Biotechnology, Santa Cruz, CA), mouse anti-lamin B1 (Abcam), mouse anti-OCT4 (Abcam), rabbit anti-K14 (Novocastra, Wetzlar, Germany), rabbit anti-TYRP1 (LifeSpan BioSciences, Seattle, WA), mouse anti-ZO-2 (Abcam), rabbit anti-Pax6 (Covance, Princeton, NJ), mouse anti-Nestin (Millipore), rabbit anti-Nestin (Millipore), rabbit anti-Sox2 (Invitrogen), rabbit anti-Tuj1 (Covance), rabbit anti-OCT4 (Santa Cruz Biotechnology), rabbit anti-TRA 1-81 (Abcam), rabbit anti-SSEA 4 (Abcam), mouse anti-ALCAM (BD Biosciences), mouse anti-Integrin β1 (BD Biosciences), mouse anti-Hyaluronate receptor (BD Biosciences), mouse anti-SH3/NT5E (BD Biosciences), rabbit anti-GFAP (Dako), mouse anti-MNR2 or HB9 (DHSB), and mouse anti-Pax3 (Millipore). Cells were stained with the species-specific fluorophore-conjugated secondary antibody (Invitrogen) (1 hr, room temperature); nuclei were visualized with DAPI. Three independent experiments were performed using each cell type. Photographs were taken using a Zeiss microscope equipped with epi-fluorescence illumination.

Flow Cytometry Analysis

Cells were detached from culture plates using Trypsin 0.05% EDTA (Invitrogen) and fixed in 4% paraformaldehyde (15 min, room temperature). After PBS wash, cells were either permeabilized with 0.1% Saponin (Sigma-Aldrich). Primary antibodies diluted at 1:100 were incubated (1 hr, room temperature) in PBS containing 0.1% FCS. Isotype-specific controls were carried out using no primary antibody. Species-specific secondary antibodies were added (1 hr, room temperature) and the cells were analyzed on a FACScalibur using CellQuest software (BD Biosciences, Franklin Lakes, NJ). The number of events analyzed for each experiment was 10,000. Three independent experiments were performed for each cell line.

Western Immunoblotting

Whole-cell lysates of MSC-iPSC were collected, separated by SDS-PAGE, and transferred onto nitrocellulose membranes by electroblotting. Blots were blocked in 10% skim milk (Bio-Rad) in Tween 0.1% Tris-buffered saline 1 hr at room temperature. The primary antibodies used were a mouse anti-lamin A/C 1:200 (Millipore, JOL2) or a β-Actin 1/200 000 (Sigma). Membranes were incubated during the night at 4°C. Antigen-antibody binding was detected using horseradish peroxidase-conjugated species-specific secondary antibodies (GE-Healthcare, Little Chalfont, UK) followed by enhanced chemiluminescence western blotting detection reagents (Perkin-Elmer, Waltham, MA). Densitometric analysis was performed and lamin A/C ratios were calculated following normalization to the value for β-Actin.

3′ UTR Luciferase Activity

Confirmation of miR-9 binding capacities to the putative 3′ UTR binding site of lamin A utilized a luciferase reporter assay. MSC-iPSC at 80% confluence were nucleofected with 1 μg of reporter vector pmiR-Target-lamin A 3′ UTR, empty vector pmiR-Target (negative transfection control) or pCMV-GFP (positive transfection control) using Amaxa nucleofector (Lonza, Basel, Switzerland). All vectors were provided by OriGene (Rockville, MD). A mutated version of pmiR-Target-lamin A 3′ UTR was obtained by directed mutagenesis, following manual instruction of QuikChange Multi-site directed mutagenesis kit (Agilent Technology). Both miR-9 recognition sites were mutated: CCAAAGA (site 1) was replaced by gCttAGA and ACCAAAG (site 2) was replaced by AgCttAG. Twenty-four hours after nucleofection, MSC-iPSC were transfected with microRNAs mimics: premiR-9, premiR-203 (unrelated negative control), premiR-Scramble (negative control or mock), anti-miR-9, or anti-miR Scramble. All premiRs and antagomiRs (Applied Biosystems) were transfected at 100 nM using lipofectamin RNAimax (Invitrogen) reagent according to manufacturer's protocol. Forty-eight hours after transfection Steady-Glo luciferase assay reagent (Promega, Madison, WI) was added to each well and the plate was incubated at room temperature in the dark for 30 min. The luciferase signal was measured using an Analyst GT counter luminometer (Molecular Devices). Data were normalized using measurement of ATP content using Cell title Glo (Promega), and knockdown was assessed by calculating luciferase signal ratios for specific miRNA/nontargeting control (mock).

microRNAs Transfection

PremiRs and antimiRs (Applied Biosystems) were transfected in MSC using lipofectamin RNAimax (Invitrogen) according to manufacturer's instructions.

Statistical Analysis

Statistical analysis has been performed by one-way analysis of variance (ANOVA), using the Dunnet's comparison test. Values of $p < 0.05$ were considered significant (*$p < 0.05$, **$p < 0.01$, ***$p < 0.001$).

SUPPLEMENTAL INFORMATION

Supplemental Information includes four figures and two tables and can be found with this article online at doi:10.1016/j.celrep.2012.05.015.

LICENSING INFORMATION

ACKNOWLEDGMENTS

The authors thank Manoubia Saidani, Céline Vallot, Drs. Jean Francois Ouimette, and Christine Baldeschi for their part in certain experiments, Claire Boissart and Dr Alexandra Benchoua for their expertise in neural cell differentiation, Dr. Susan Cure for revising the manuscript, and Drs. Walter Habeler, Alexandre Méjat, Claire Rougeulle, and Pierre Cau for providing helpful discussions. This work was supported by the Institut National de la Santé et de la Recherche Médicale (INSERM), University Evry Val d'Essonne (UEVE), Association Française contre les Myopathies (AFM), and Genopole.

Received: November 30, 2011
Revised: April 24, 2012
Accepted: May 18, 2012
Published online: June 21, 2012

REFERENCES

Ambasudhan, R., Talantova, M., Coleman, R., Yuan, X., Zhu, S., Lipton, S.A., and Ding, S. (2011). Direct reprogramming of adult human fibroblasts to functional neurons under defined conditions. Cell Stem Cell *9*, 113–118.

Bartel, D.P. (2009). MicroRNAs: target recognition and regulatory functions. Cell *136*, 215–233.

Boissart, C., Nissan, X., Giraud-Triboult, K., Peschanski, M., and Benchoua, A. (2012). miR-125 potentiates early neural specification of human embryonic stem cells. Development *139*, 1247–1257.

Burke, B., and Stewart, C.L. (2006). The laminopathies: the functional architecture of the nucleus and its contribution to disease. Annu. Rev. Genomics Hum. Genet. *7*, 369–405.

Cao, K., Graziotto, J.J., Blair, C.D., Mazzulli, J.R., Erdos, M.R., Krainc, D., and Collins, F.S. (2011). Rapamycin reverses cellular phenotypes and enhances mutant protein clearance in Hutchinson-Gilford progeria syndrome cells. Sci. Transl. Med. *3*, 89ra58.

Chambers, S.M., Fasano, C.A., Papapetrou, E.P., Tomishima, M., Sadelain, M., and Studer, L. (2009). Highly efficient neural conversion of human ES and iPS cells by dual inhibition of SMAD signaling. Nat. Biotechnol. *27*, 275–280.

Columbaro, M., Capanni, C., Mattioli, E., Novelli, G., Parnaik, V.K., Squarzoni, S., Maraldi, N.M., and Lattanzi, G. (2005). Rescue of heterochromatin

organization in Hutchinson-Gilford progeria by drug treatment. Cell. Mol. Life Sci. *62*, 2669–2678.

De Pietri Tonelli, D., Pulvers, J.N., Haffner, C., Murchison, E.P., Hannon, G.J., and Huttner, W.B. (2008). miRNAs are essential for survival and differentiation of newborn neurons but not for expansion of neural progenitors during early neurogenesis in the mouse embryonic neocortex. Development *135*, 3911–3921.

De Sandre-Giovannoli, A., Bernard, R., Cau, P., Navarro, C., Amiel, J., Boccaccio, I., Lyonnet, S., Stewart, C.L., Munnich, A., Le Merrer, M., and Lévy, N. (2003). Lamin a truncation in Hutchinson-Gilford progeria. Science *300*, 2055.

Delaloy, C., Liu, L., Lee, J.A., Su, H., Shen, F., Yang, G.Y., Young, W.L., Ivey, K.N., and Gao, F.B. (2010). MicroRNA-9 coordinates proliferation and migration of human embryonic stem cell-derived neural progenitors. Cell Stem Cell *6*, 323–335.

Eriksson, M., Brown, W.T., Gordon, L.B., Glynn, M.W., Singer, J., Scott, L., Erdos, M.R., Robbins, C.M., Moses, T.Y., Berglund, P., et al. (2003). Recurrent de novo point mutations in lamin A cause Hutchinson-Gilford progeria syndrome. Nature *423*, 293–298.

Giraud-Triboult, K., Rochon-Beaucourt, C., Nissan, X., Champon, B., Aubert, S., and Piétu, G. (2011). Combined mRNA and microRNA profiling reveals that miR-148a and miR-20b control human mesenchymal stem cell phenotype via EPAS1. Physiol. Genomics *43*, 77–86.

Goldman, R.D., Shumaker, D.K., Erdos, M.R., Eriksson, M., Goldman, A.E., Gordon, L.B., Gruenbaum, Y., Khuon, S., Mendez, M., Varga, R., and Collins, F.S. (2004). Accumulation of mutant lamin A causes progressive changes in nuclear architecture in Hutchinson-Gilford progeria syndrome. Proc. Natl. Acad. Sci. USA *101*, 8963–8968.

Guenou, H., Nissan, X., Larcher, F., Feteira, J., Lemaitre, G., Saidani, M., Del Rio, M., Barrault, C.C., Bernard, F.X., Peschanski, M., et al. (2009). Human embryonic stem-cell derivatives for full reconstruction of the pluristratified epidermis: a preclinical study. Lancet *374*, 1745–1753.

Hennekam, R.C. (2006). Hutchinson-Gilford progeria syndrome: review of the phenotype. Am. J. Med. Genet. A. *140*, 2603–2624.

Ho, J.C., Zhou, T., Lai, W.H., Huang, Y., Chan, Y.C., Li, X., Wong, N.L., Li, Y., Au, K.W., Guo, D., et al. (2011). Generation of induced pluripotent stem cell lines from 3 distinct laminopathies bearing heterogeneous mutations in lamin A/C. Aging (Albany NY) *3*, 380–390.

Houbaviy, H.B., Murray, M.F., and Sharp, P.A. (2003). Embryonic stem cell-specific MicroRNAs. Dev. Cell *5*, 351–358.

Huang, S., Chen, L., Libina, N., Janes, J., Martin, G.M., Campisi, J., and Oshima, J. (2005). Correction of cellular phenotypes of Hutchinson-Gilford Progeria cells by RNA interference. Hum. Genet. *118*, 444–450.

Judson, R.L., Babiarz, J.E., Venere, M., and Blelloch, R. (2009). Embryonic stem cell-specific microRNAs promote induced pluripotency. Nat. Biotechnol. *27*, 459–461.

Jung, H.J., Coffinier, C., Choe, Y., Beigneux, A.P., Davies, B.S., Yang, S.H., Barnes, R.H., 2nd, Hong, J., Sun, T., Pleasure, S.J., et al. (2012). Regulation of prelamin A but not lamin C by miR-9, a brain-specific microRNA. Proc. Natl. Acad. Sci. USA *109*, E423–E431.

Krichevsky, A.M., Sonntag, K.C., Isacson, O., and Kosik, K.S. (2006). Specific microRNAs modulate embryonic stem cell-derived neurogenesis. Stem Cells *24*, 857–864.

Lee, R., Feinbaum, R., and Ambros, V. (2004). A short history of a short RNA. Cell *116*, S89–S92, 1 p following S96.

Lee, R.C., Feinbaum, R.L., and Ambros, V. (1993). The C. elegans heterochronic gene lin-4 encodes small RNAs with antisense complementarity to lin-14. Cell *75*, 843–854.

Lehner, C.F., Stick, R., Eppenberger, H.M., and Nigg, E.A. (1987). Differential expression of nuclear lamin proteins during chicken development. J. Cell Biol. *105*, 577–587.

Leucht, C., Stigloher, C., Wizenmann, A., Klafke, R., Folchert, A., and Bally-Cuif, L. (2008). MicroRNA-9 directs late organizer activity of the midbrain-hindbrain boundary. Nat. Neurosci. *11*, 641–648.

Liu, B., Wang, J., Chan, K.M., Tjia, W.M., Deng, W., Guan, X., Huang, J.D., Li, K.M., Chau, P.Y., Chen, D.J., et al. (2005). Genomic instability in laminopathy-based premature aging. Nat. Med. *11*, 780–785.

Liu, G.H., Barkho, B.Z., Ruiz, S., Diep, D., Qu, J., Yang, S.L., Panopoulos, A.D., Suzuki, K., Kurian, L., Walsh, C., et al. (2011a). Recapitulation of premature ageing with iPSCs from Hutchinson-Gilford progeria syndrome. Nature *472*, 221–225.

Liu, G.H., Suzuki, K., Qu, J., Sancho-Martinez, I., Yi, F., Li, M., Kumar, S., Nivet, E., Kim, J., Soligalla, R.D., et al. (2011b). Targeted gene correction of laminopathy-associated LMNA mutations in patient-specific iPSCs. Cell Stem Cell *8*, 688–694.

Mariño, G., Ugalde, A.P., Fernández, A.F., Osorio, F.G., Fueyo, A., Freije, J.M., and López-Otín, C. (2010). Insulin-like growth factor 1 treatment extends longevity in a mouse model of human premature aging by restoring somatotroph axis function. Proc. Natl. Acad. Sci. USA *107*, 16268–16273.

Merideth, M.A., Gordon, L.B., Clauss, S., Sachdev, V., Smith, A.C., Perry, M.B., Brewer, C.C., Zalewski, C., Kim, H.J., Solomon, B., et al. (2008). Phenotype and course of Hutchinson-Gilford progeria syndrome. N. Engl. J. Med. *358*, 592–604.

Misteli, T., and Scaffidi, P. (2005). Genome instability in progeria: when repair gets old. Nat. Med. *11*, 718–719.

Navarro, C.L., Cau, P., and Lévy, N. (2006). Molecular bases of progeroid syndromes. Hum. Mol. Genet. *15* (Spec No 2), R151–R161.

Nissan, X., Denis, J.A., Saidani, M., Lemaitre, G., Peschanski, M., and Baldeschi, C. (2011a). miR-203 modulates epithelial differentiation of human embryonic stem cells towards epidermal stratification. Dev. Biol. *356*, 506–515.

Nissan, X., Larribere, L., Saidani, M., Hurbain, I., Delevoye, C., Feteira, J., Lemaitre, G., Peschanski, M., and Baldeschi, C. (2011b). Functional melanocytes derived from human pluripotent stem cells engraft into pluristratified epidermis. Proc. Natl. Acad. Sci. USA *108*, 14861–14866.

Osorio, F.G., Navarro, C.L., Cadinanos, J., Lopez-Mejia, I.C., Quiros, P.M., Bartoli, C., Rivera, J., Tazi, J., Guzman, G., Varela, I., et al. (2011). Splicing-directed therapy in a new mouse model of human accelerated aging. Sci. Transl. Med. *3*, 106ra107.

Paradisi, M., McClintock, D., Boguslavsky, R.L., Pedicelli, C., Worman, H.J., and Djabali, K. (2005). Dermal fibroblasts in Hutchinson-Gilford progeria syndrome with the lamin A G608G mutation have dysmorphic nuclei and are hypersensitive to heat stress. BMC Cell Biol. *6*, 27.

Röber, R.A., Weber, K., and Osborn, M. (1989). Differential timing of nuclear lamin A/C expression in the various organs of the mouse embryo and the young animal: a developmental study. Development *105*, 365–378.

Ruvkun, G. (2001). Molecular biology. Glimpses of a tiny RNA world. Science *294*, 797–799.

Smirnova, L., Gräfe, A., Seiler, A., Schumacher, S., Nitsch, R., and Wulczyn, F.G. (2005). Regulation of miRNA expression during neural cell specification. Eur. J. Neurosci. *21*, 1469–1477.

Suh, M.R., Lee, Y., Kim, J.Y., Kim, S.K., Moon, S.H., Lee, J.Y., Cha, K.Y., Chung, H.M., Yoon, H.S., Moon, S.Y., et al. (2004). Human embryonic stem cells express a unique set of microRNAs. Dev. Biol. *270*, 488–498.

Takahashi, K., Tanabe, K., Ohnuki, M., Narita, M., Ichisaka, T., Tomoda, K., and Yamanaka, S. (2007). Induction of pluripotent stem cells from adult human fibroblasts by defined factors. Cell *131*, 861–872.

Townley-Tilson, W.H., Callis, T.E., and Wang, D. (2010). MicroRNAs 1, 133, and 206: critical factors of skeletal and cardiac muscle development, function, and disease. Int. J. Biochem. Cell Biol. *42*, 1252–1255.

Ugalde, A.P., Ramsay, A.J., de la Rosa, J., Varela, I., Mariño, G., Cadiñanos, J., Lu, J., Freije, J.M., and López-Otín, C. (2011). Aging and chronic DNA damage response activate a regulatory pathway involving miR-29 and p53. EMBO J. *30*, 2219–2232.

Vasilatou, D., Papageorgiou, S., Pappa, V., Papageorgiou, E., and Dervenoulas, J. (2010). The role of microRNAs in normal and malignant hematopoiesis. Eur. J. Haematol. *84*, 1–16.

Yi, R., O'Carroll, D., Pasolli, H.A., Zhang, Z., Dietrich, F.S., Tarakhovsky, A., and Fuchs, E. (2006). Morphogenesis in skin is governed by discrete sets of differentially expressed microRNAs. Nat. Genet. *38*, 356–362.

Yi, R., Poy, M.N., Stoffel, M., and Fuchs, E. (2008). A skin microRNA promotes differentiation by repressing 'stemness'. Nature *452*, 225–229.

Yoo, A.S., Staahl, B.T., Chen, L., and Crabtree, G.R. (2009). MicroRNA-mediated switching of chromatin-remodelling complexes in neural development. Nature *460*, 642–646.

Zhang, J., Lian, Q., Zhu, G., Zhou, F., Sui, L., Tan, C., Mutalif, R.A., Navasankari, R., Zhang, Y., Tse, H.F., et al. (2011). A human iPSC model of Hutchinson Gilford Progeria reveals vascular smooth muscle and mesenchymal stem cell defects. Cell Stem Cell *8*, 31–45.

Zhao, C., Sun, G., Li, S., and Shi, Y. (2009). A feedback regulatory loop involving microRNA-9 and nuclear receptor TLX in neural stem cell fate determination. Nat. Struct. Mol. Biol. *16*, 365–371.